Src kinase activity and SH2 domain regulate the dynamics of Src association with lipid and protein targets

Dmitry E. Shvartsman,[1] John C. Donaldson,[2] Begoña Diaz,[2] Orit Gutman,[1] G. Steven Martin,[2] and Yoav I. Henis[1]

[1]Department of Neurobiochemistry, George S. Wise Faculty of Life Sciences, Tel Aviv University, Tel Aviv 69978, Israel
[2]Department of Molecular and Cell Biology, University of California at Berkeley, Berkeley, CA 94720

Src functions depend on its association with the plasma membrane and with specific membrane-associated assemblies. Many aspects of these interactions are unclear. We investigated the functions of kinase, SH2, and SH3 domains in Src membrane interactions. We used FRAP beam-size analysis in live cells expressing a series of c-Src–GFP proteins with targeted mutations in specific domains together with biochemical experiments to determine whether the mutants can generate and bind to phosphotyrosyl proteins. Wild-type Src displays lipid-like membrane association, whereas constitutively active Src-Y527F interacts transiently with slower-diffusing membrane-associated proteins. These interactions require Src kinase activity and SH2 binding, but not SH3 binding. Furthermore, overexpression of paxillin, an Src substrate with a high cytoplasmic population, competes with membrane phosphotyrosyl protein targets for binding to activated Src. Our observations indicate that the interactions of Src with lipid and protein targets are dynamic and that the kinase and SH2 domain cooperate in the membrane targeting of Src.

Introduction

Cellular c-Src (Src) is a nonreceptor protein tyrosine kinase associated with the plasma membrane, cell–matrix and cell–cell adhesions, and endosomal vesicles. It mediates signaling by a variety of receptors (Schlaepfer et al., 1999; Abram and Courtneidge, 2000). Constitutively active Src can elicit cell transformation in vitro (Martin, 2001; Courtneidge, 2002; Frame, 2004), and Src expression and activity are elevated in many human epithelial cancers (Bjorge et al., 2000). The first 16 N-terminal residues of Src (residue numbers refer to chicken c-Src) contain an *N*-myristoylation site and a series of basic residues, both required for membrane association (Resh, 1999). Residues 17–84 constitute a unique domain, followed by SH3 and SH2 domains connected by a short linker. Another linker connects the SH2 domain to the kinase domain, which is required for most biological functions of Src. Tyr527 (or Tyr530 in human Src) undergoes an inhibitory phosphorylation by C-terminal Src kinase. In the inactive or "closed" form of Src, the SH2 domain interacts with pTyr527, positioning the SH3 domain to interact with a polyproline type II helix in the kinase-SH2 linker region. This causes inactivating conformational changes in the N-lobe of the kinase. Activation can occur as a result of dephosphorylation or mutation of Tyr527 or by binding of the SH2 or SH3 domains to activating ligands (Martin, 2001; Courtneidge, 2002; Frame, 2004; Chong et al., 2005).

Src initiates intracellular signaling by binding to protein substrates via its SH3 and SH2 domains, often inducing their processive phosphorylation. For example, Src SH3-dependent binding to p130Cas initiates a tyrosine phosphorylation cascade, in which the initially formed phosphotyrosyl (pTyr) residue binds to the Src SH2 domain, followed by phosphorylation at additional sites (Mayer et al., 1995). Thus, Src SH3 and SH2 domains have dual roles, mediating inactivating intramolecular interactions as well as promoting substrate phosphorylation.

Membrane association is critical for Src signaling, as indicated by the finding that a mutation eliminating myristoylation blocks cell transformation by activated Src (Kamps et al., 1985; Buss et al., 1986). Other Src-family kinases (SFKs), such as Fyn, Yes, and Lck, are thought to reside in cholesterol-enriched

D.E. Shvartsman and J.C. Donaldson contributed equally to this work.

Correspondence to Yoav I. Henis: henis@post.tau.ac.il

B. Diaz's present address is Centro Nacional de Investigaciones Oncológicas, E-28029 Madrid, Spain.

Abbreviations used in this paper: SFK, Src-family kinase; TM, transmembrane; WT, wild-type.

The online version of this article contains supplemental material.

The Journal of Cell Biology, Vol. 178, No. 4, August 13, 2007 675–686
http://www.jcb.org/cgi/doi/10.1083/jcb.200701133

assemblies (commonly referred to as lipid rafts) and caveolae by virtue of their dual acylation (Shenoy-Scaria et al., 1994; Robbins et al., 1995; Resh, 1999; Janes et al., 2000). However, the single myristoyl in Src is not considered a strong raft-targeting signal (Melkonian et al., 1999), and reports on the raft association of Src were ambiguous (Shenoy-Scaria et al., 1994; Tansey et al., 2000; Lee et al., 2002; Mukherjee et al., 2003; Chen et al., 2006; Veracini et al., 2006).

Despite the functional importance of Src membrane association, little is known about the dynamics of these interactions, and how different elements (the kinase, SH2, and SH3 domains) control Src membrane targeting and association with substrate proteins. We tackled these questions by studying a series of chicken c-Src mutants fused to GFP, combining FRAP beam-size analysis (Henis et al., 2006) to determine their membrane association with biochemical studies to characterize their interactions with pTyr protein targets. Our data demonstrate that wild-type (WT) Src displays lipid-like membrane association, whereas the open-conformation constitutively active Src-Y527F shows a substantial contribution of interactions with slower-diffusing membrane-associated proteins. These interactions depend mutually on Src kinase activity and SH2 domain binding. The results suggest distinct and novel roles for Src kinase activity and SH2 and SH3 domains in regulating Src membrane interactions.

Table I. **Src-GFP mutants**

Src mutant	Description
Src-WT-GFP	WT chicken c-Src
Src-K295M-GFP	Kinase-dead mutant
Src-Y527F-GFP	Y527F mutation, open conformation, constitutively active
Src-Y527F/K295M-GFP	Double mutant, open conformation, kinase dead
Src-Y527F/R175A-GFP	Double mutant, open conformation, inactivated SH2 domain
Src-Y527F/W118A-GFP	Double mutant, open conformation, inactivated SH3 domain
Src-Y527F/K295M/ R175A-GFP	Triple mutant, open conformation, kinase dead, inactivated SH2
Src-251-GFP	Truncated N-terminal half, containing SH3/SH2 domains, no kinase region

Table shows Src-GFP constructs used in the studies. Chicken c-Src-WT-GFP was shown to undergo normal regulation in cells; Src-Y527F-GFP and Src-251-GFP were demonstrated to be active and possess correct cellular localization (Timpson et al., 2001; Sandilands et al., 2004). Additional mutants were constructed by site-directed mutagenesis using Src-WT-GFP or Src-Y527F-GFP as templates; the Y527F/K295M double mutant served as a template for the triple mutant. All constructs are in pEGFP-N1, except Src-251-GFP (pBabePuro). The K295M mutation inactivates Src kinase activity (Kamps et al., 1984; Kamps and Sefton, 1986), the R175A mutation inactivates pTyr binding by the SH2 domain (Waksman et al., 1993), and the W118A mutation inactivates SH3 domain binding (Musacchio et al., 1994; Erpel et al., 1995).

Results

Interactions with membrane proteins contribute to the membrane association of activated but not nonactivated Src

To study the roles of Src kinase activity and SH3 and SH2 domains in its interactions with the plasma membrane, we combined biochemical studies with FRAP beam-size analysis in live cells (Illenberger et al., 2003; Henis et al., 2006). The latter approach characterizes the membrane interactions of inner-leaflet proteins based on their lateral diffusion rates and on the relative contribution of exchange between membrane and cytosolic pools to their FRAP. These studies used a series of mutants of chicken c-Src with GFP fused at the C terminus (Table I).

To investigate whether Src activation affects its distribution between cytosolic and membrane fractions, we transfected COS-7 cells with Src-WT-GFP or constitutively active Src-Y527F-GFP and compared their membrane association by cell fractionation (Fig. 1) and FRAP (Figs. 2 and 3). Src-WT-GFP and Src-Y527F-GFP displayed a twofold higher percentage in the particulate (membrane) fraction (Fig. 1 A). The percentage of Src-Y527F-GFP in the membrane was slightly higher, possibly reflecting interactions with membrane-associated protein structures (e.g., focal adhesions) and peripheral membranes (Kaplan et al., 1994; Sandilands et al., 2004); this is in accord with the appearance of Src-Y527F-GFP in more distinct clusters, which partially colocalize with vinculin (Fig. 1 B).

To characterize the interactions of Src-GFP proteins with the plasma membrane, we conducted FRAP studies on live cells expressing Src-WT-GFP and Src-Y527F-GFP. Typical experiments are shown in Fig. 2; quantitative results on multiple cells using two different laser beam sizes (beam-size analysis) are depicted in Fig. 3. The beam-size analysis (Henis et al., 2006) explores membrane interactions of proteins interacting with the inner membrane leaflet, where FRAP can occur not only by lateral diffusion but also by exchange between membrane and cytoplasmic pools. If FRAP occurs solely by lateral diffusion, the characteristic fluorescence recovery time τ ($t_{1/2}$ for recovery) is the characteristic diffusion time, τ_D, proportional to the area illuminated by the beam ($\tau = \tau_D = \omega^2/4D$, where ω is the Gaussian radius of the beam and D is the lateral diffusion coefficient; Petersen et al., 1986). When FRAP occurs by exchange, τ is the chemical relaxation time, which is independent of the beam size (Henis et al., 2006). The $\tau(40\times)/\tau(63\times)$ ratio expected for the two beam sizes generated using the 40× and 63× objectives is 2.56 (the measured ratio between the illuminated areas) for recovery by pure lateral diffusion, versus 1 for exchange; intermediate values suggest a mixed recovery mode, where the faster process has a higher contribution (Henis et al., 2006).

In the current studies, we focused the laser beam on the nonadherent plasma membrane away from potential cell-substrate contacts, although for the coverslip-attached COS cells (few focal adhesions), similar results were obtained on the adherent membranes. FRAP of a free cytoplasmic protein (GFP) was faster than the experimental time scale, ensuring that fast cytoplasmic diffusion does not contribute to the measurement (Fig. 2 A). In accord with the fractionation experiments, which demonstrated both membrane and cytoplasmic pools, the beam-size analysis yielded $\tau(40\times)/\tau(63\times) = 1.8$ for Src-WT-GFP (FRAP by mixed lateral diffusion and exchange; Fig. 3). The contribution of exchange precludes an accurate translation of τ to D, but D can be estimated from $\tau(63\times)$, because the smaller beam area reduces the characteristic diffusion time τ_D; as τ for

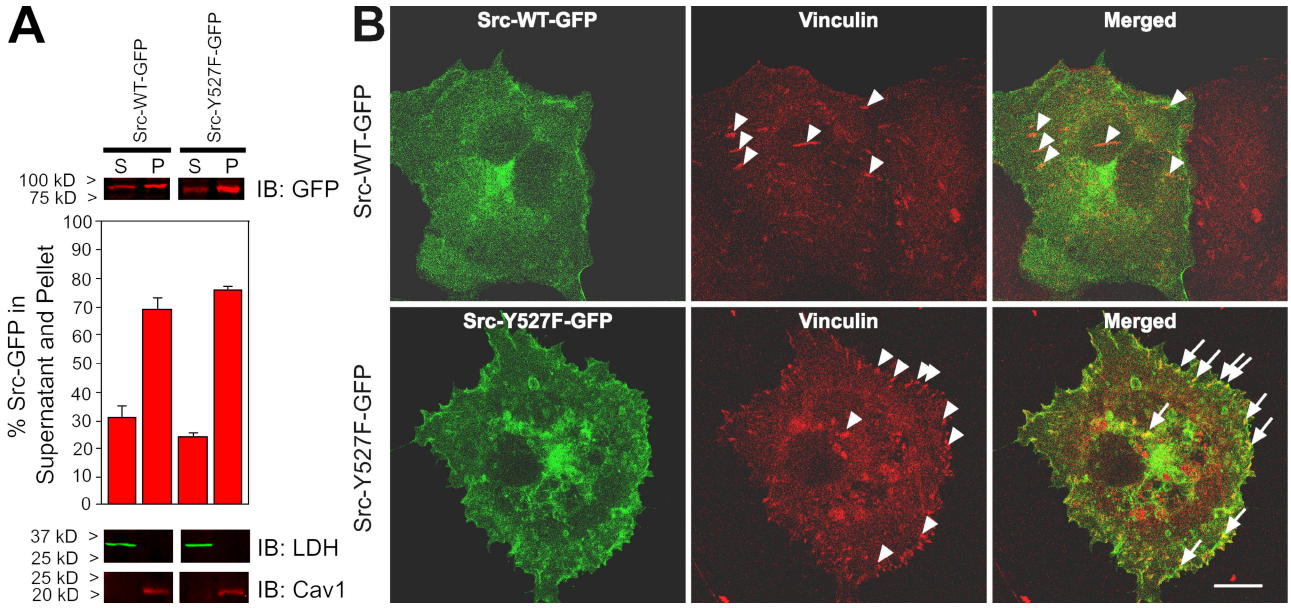

Figure 1. **Membrane association and cellular distribution of Src-WT-GFP and Src-Y527F-GFP.** COS-7 cells were transfected with one of the above constructs as described under Materials and methods. (A) Percentage of Src-GFP in supernatant (S; cytosol) and pellet (P; membrane). After subcellular fractionation, equal proportions (5% vol/vol) of each fraction were quantified by immunoblotting. The immunoblot (IB) panels (blotting for GFP to identify Src-GFP proteins or for lactate dehydrogenase [LDH] and caveolin1 [Cav1] as cytosolic and membrane markers, respectively) are from a representative experiment, whereas the bar graph shows means ± SEM (n = 3) of multiple experiments. The percentage of Src-Y527F-GFP in pellet was somewhat higher, but the difference was not significant ($P > 0.05$; t test). (B) Cellular distribution of Src-WT-GFP and Src-Y527F-GFP. Transfected cells were fixed, permeabilized, and immunostained for vinculin (1:100 dilution of mouse anti-vinculin ascites, followed by 30 μg/ml Cy3 goat anti–mouse IgG). Fluorescence confocal imaging was as described in Materials and methods. Arrowheads point at vinculin (red) in focal adhesions; arrows indicate colocalization of Src (observed for Src-Y527F-GFP but not for Src-WT-GFP) with vinculin. Bar, 10 μm.

exchange does not depend on the beam size, this results in a higher contribution of lateral diffusion to the recovery with the smaller beam size (Henis et al., 2006). This yields $D = 0.57$ μm^2/s (Fig. 2 B and Fig. 3 A) for Src-WT, close to D determined by fluorescence correlation spectroscopy (Larson et al., 2005) for the dually acylated SFK Lyn-GFP (0.3 μm^2/s) and to the D value we have measured for a lipid probe (DiIC$_{16}$; 1 μm^2/s) in COS-7 cells (Rotblat et al., 2004). The membrane association of Src-WT-GFP is therefore mediated mainly by lipid-like interactions, presumably via its myristoyl residue and N-terminal region. On the other hand, constitutively active Src-Y527F-GFP exhibited markedly slower FRAP rates and a minor increase in the τ(40×)/τ(63×) ratio to 2.2 (Fig. 2 C and Fig. 3). An elevated τ ratio suggests that the exchange rate is slowed relative to the lateral diffusion, in line with the slightly higher membrane fraction of Src-Y527F-GFP (Fig. 1 A). Yet, both τ(63×) and τ(40×) of Src-Y527F were strongly elevated, indicating that both exchange and lateral diffusion are inhibited, with a somewhat stronger effect on the exchange rate. Calculating D of Src-Y527F-GFP from τ(63×) yields $D = 0.20$ μm^2/s (Fig. 2 C and Fig. 3 A), approximately fivefold slower than the lipid probe. This suggests that interactions with transmembrane (TM) and/or membrane-associated proteins (whose lateral diffusion is slower than lipids) considerably contribute to the membrane association of Src-Y527F. The observed differences between Src-Y527F and Src-WT are not due to effects of Src activity on the membrane, as overexpression of constitutively active human c-Src-Y530F (10-fold excess plasmid DNA over Src-WT-GFP) did not affect the FRAP parameters of Src-WT-GFP (unpublished data).

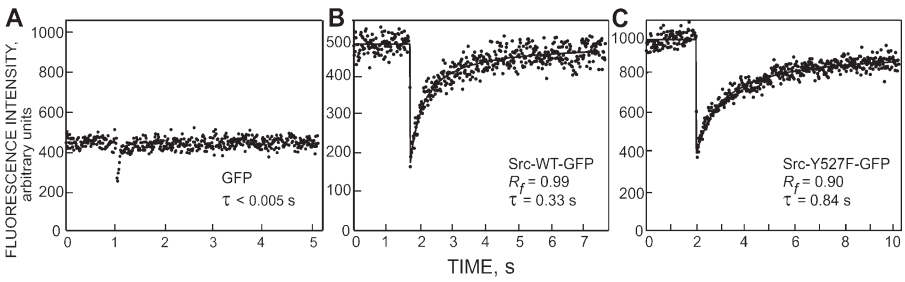

Figure 2. **Typical curves showing that the FRAP rate of Src-Y527F-GFP is slow relative to that of Src-WT-GFP.** FRAP experiments were conducted at 22°C on COS-7 cells transiently expressing EGFP (GFP; A), Src-WT-GFP (B), or Src-Y527F-GFP (C), using the 63× objective (see Materials and methods). Solid lines show the best fit of a nonlinear regression analysis, with the resulting τ and mobile fraction (R_f) values. (A) Free GFP recovers instantaneously on the experimental time scale, demonstrating that free diffusion in the cytoplasm does not contribute to the measurements in the other panels. (B and C) Src-WT-GFP displays slower FRAP enabling measurement of τ, whereas Src-Y527F-GFP exhibits a further notable reduction in the recovery kinetics.

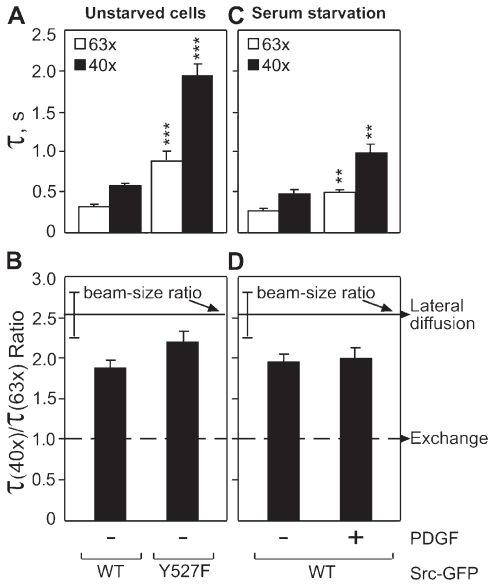

Figure 3. **FRAP beam-size analysis of the membrane interactions of Src-WT-GFP and Src-Y527F-GFP.** FRAP experiments were conducted as in Fig. 2 on cells grown with 10% FCS (A and B) or on serum-starved cells with or without PDGF stimulation (C and D). Bars are means ± SEM of 40–60 measurements. Two beam sizes were generated using 63× and 40× objectives, and the τ values were determined with each. The ratio between the areas illuminated by the two beams was 2.56 ± 0.30 (n = 39); this ratio (B and D, solid lines) is expected for FRAP by lateral diffusion, whereas a ratio of 1 (broken lines) is expected for recovery by exchange (Henis et al., 2006). The R_f values were high in all cases (averaging 0.98 for Src-WT-GFP and 0.92 for Src-Y527F-GFP). (A) τ values in unstarved cells. The differences between the τ(63×) or τ(40×) values of Src-Y527F and Src-WT were highly significant, comparing the two proteins with the same beam size (***, $P < 10^{-17}$; t test). (B) τ(40×)/τ(63×) ratios in unstarved cells. The τ ratio of Src-WT-GFP (but not of Src-Y527F-GFP) differed significantly from the 2.56 ratio between the measured beam sizes ($P < 0.005$). (C) Effects of serum starvation and PDGF on the τ values of Src-WT-GFP. PDGF stimulation (see Materials and methods) significantly increased the τ values of Src-WT (**, $P < 10^{-9}$). (D) τ(40×)/τ(63×) ratios derived from C. Both τ ratios are significantly below the 2.56 beam-size ratio ($P < 0.05$).

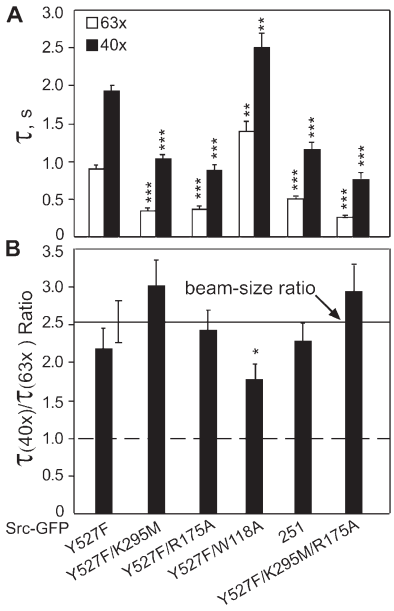

Figure 4. **FRAP studies demonstrate distinct roles for Src kinase activity and SH2 and SH3 domains in Src membrane interactions.** FRAP experiments were conducted as in Fig. 3. Results are mean ± SEM of 40–60 measurements. The R_f values were high in all cases (≥0.92; not depicted). (A) τ values. Asterisks indicate significant differences from τ(63×) or τ(40×) measured for Src-Y527F-GFP (**, $P < 0.001$; ***, $P < 10^{-7}$). (B) τ(40×)/τ(63×) ratios. Only the τ(40×)/τ(63×) ratio of Src-Y527F/W118A is significantly different from 2.56 ± 0.3 (*, $P < 0.005$). The D values calculated for the various mutants are given in the text.

The aforementioned experiments were conducted on cells grown with 10% FCS, conditions that may activate part of the Src-WT population. However, the percentage of activated Src-WT molecules is low, as indicated by the small (although significant; $P < 0.02$, t test) effect of serum starvation on τ(63×) and τ(40×) of Src-WT-GFP (Fig. 3). The slight increase in the FRAP rate of Src-WT under these conditions (to $D = 0.72$ μm²/s, as calculated from τ[63×]), together with the lack of effect on the τ values of constitutively active Src-Y527F-GFP (unpublished data), suggests that only a minor fraction of Src-WT is activated in cells grown continuously in the presence of serum. Accordingly, all the FRAP parameters of Src-WT in the presence of serum were similar to those of the kinase-dead Src-K295M mutant ($P > 0.2$). Therefore, as serum starvation may induce apoptosis, further comparisons between Src-GFP mutants were conducted on unstarved cells.

Importantly, activation of Src-WT-GFP in serum-starved cells by PDGF significantly increased the τ values of Src-WT-GFP, suggesting a retardation in the FRAP kinetics (Fig. 3 C). This effect is in the same direction as that induced by the constitutively activating mutation (Y527F) but is considerably milder; this is not surprising considering the modest activation of Src-WT in PDGF-treated cells (Abram and Courtneidge, 2000; Sandilands et al., 2004).

The mobility-restricting interactions of Src-Y527F-GFP with the plasma membrane depend mainly on its kinase activity and SH2 domain

To explore the roles of Src kinase activity and SH2 and SH3 domains in the membrane association of Src-Y527F, we used FRAP beam-size analysis to investigate a series of Src-GFP mutants (Fig. 4). Inactivating Src kinase by a second mutation in Src-Y527F (Src-Y527F/K295M) strongly reduced τ(63×) and τ(40×), bringing them close to those of Src-WT (Fig. 4 A). Analogous effects followed SH2 inactivation (Src-Y527F/R175A) or deletion of the kinase domain (Src-251). Calculation of D from τ(63×) shows that these mutants revert to lipid-like diffusion (D ~0.5 μm²/s). The triple mutant Src-Y527F/K295M/R175A, which lacks both kinase activity and SH2 binding, exhibited somewhat faster FRAP rates than Src-Y527F/K295M or Src-251 ($D = 0.72$ μm²/s); the latter two possess an exposed SH2 domain that can bind pTyr residues generated by endogenous SFKs. In contrast, SH3 domain inactivation (Src-Y527F/W118A) did not enhance the FRAP rates and mildly increased τ(63×) and τ(40×) (Fig. 4 A). The further retardation ($D = 0.13$ μm²/s; calculated from τ[63×]) suggests enhanced interactions with slower-diffusing membrane proteins. Collectively, these findings suggest that the mobility-restricting membrane interactions of Src-Y527F depend on its kinase activity and SH2

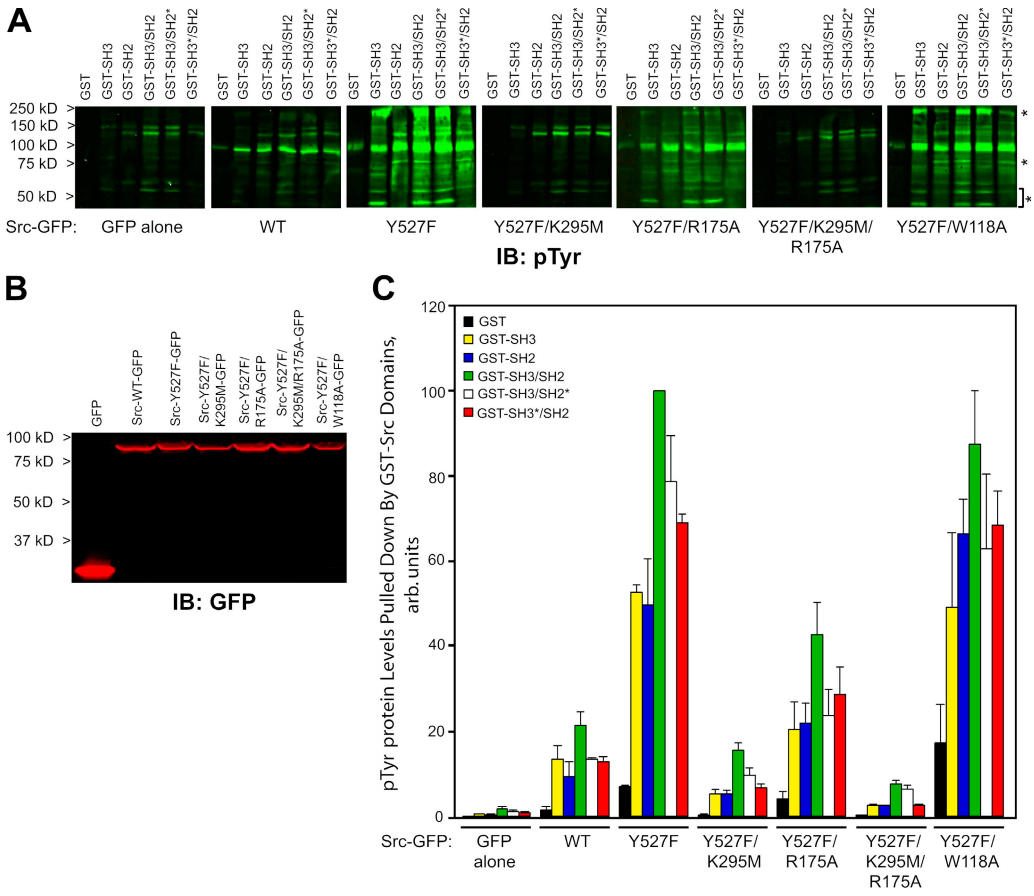

Figure 5. **Binding of pTyr proteins from cells expressing Src-GFP mutants to GST-Src domain fusion proteins.** COS-7 cells were transfected with vectors encoding different Src-GFP proteins or GFP (control) and lysed (see Materials and methods). After protein and Src-GFP level determination, 6 aliquots (0.5 mg protein) from each lysate were precipitated by GST-Src domain fusion proteins coupled to glutathione–Sepharose beads, followed by 8.5% SDS-PAGE and immunoblotting. The GST-Src domain constructs (see Table S2, available at http://www.jcb.org/cgi/content/full/jcb.200701133/DC1) were as follows: GST-SH3, GST-SH2, GST-SH3/SH2 (including both domains), GST-SH3/SH2* (SH2 with R175A mutation), and GST-SH3*/SH2 (SH3 with W118A mutation). A and B depict a representative experiment, whereas C gives the means ± SEM ($n = 3$) of multiple experiments. (A) Typical blots of pTyr proteins precipitated from cells transfected with the indicated Src-GFP plasmids. Blots were probed with mouse anti-pTyr followed by IRDye 800 goat anti–mouse IgG. Although many pTyr proteins are precipitated by both GST-SH2 and GST-SH3, presumably because they contain binding sites for both, some are precipitated selectively by one but not the other (right, asterisks). (B) Expression levels of the Src-GFP proteins in the cells shown in A. From each lysate, 25 μg protein was resolved by 8.5% SDS-PAGE and immunoblotted with rabbit anti-GFP and Alexa 680 goat anti–rabbit IgG. (C) Quantification of precipitated pTyr proteins. Results are mean ± SEM of three experiments. For each lane shown in A, the sum of the intensities of all bands (the cumulative pTyr precipitated by a specific GST fusion protein) was calibrated according to the Src-GFP level in the same transfection (B). The results are presented relative to the calibrated level of pTyr proteins precipitated by GST-SH3/SH2 from cells transfected with Src-Y527F-GFP within each set of experiments, taking this value as 100.

binding, whereas SH3 binding is dispensable. This does not imply that the SH3 domain cannot bind Src target proteins (Fig. 5 C); however, the generally lower binding affinities of Src SH3 relative to SH2 (Li, 2005; Liu et al., 2006) may render SH3 binding ineffective in retarding the diffusion of Src-Y527F. Moreover, the conformational change mediated by the SH3-inactivating mutation enhances Src kinase activity (Kanner et al., 1991; Erpel et al., 1995; Chong et al., 2005), potentially compensating for the loss of SH3 binding by generating more pTyr residues that can enhance Src binding via the SH2 domain. This could lead to the additional increase in $\tau(63\times)$ and $\tau(40\times)$ observed for Src-Y527F/W118A (Fig. 4). The SH2 mutation (R175A), in contrast, does not affect the catalytic activity of Src-Y527F because the intramolecular interaction between the SH2 domain and the C-terminal region is already disrupted by the Y527F mutation (Superti-Furga and Gonfloni, 1997).

All Src-GFP mutants except Src-Y527F/W118A exhibited τ ratios not significantly different from the 2.56 ± 0.3 ratio expected for recovery by lateral diffusion, suggesting low contribution of exchange. This contrasts with Src-WT, whose τ ratio was significantly below 2.56 ($P < 0.005$; Fig. 3 B). Thus, shifting to an open conformation may have a minor effect on the insertion of the N-terminal anchor of Src in the membrane. Unlike Src-Y527F, the τ ratio of Src-Y527F/W118A was significantly lower than 2.56 ($P < 0.005$; Fig. 4 B), suggesting a higher relative contribution of exchange. A simple explanation may be that SH3 domain binding (lost in this mutant) retards mainly the exchange kinetics. However, because the τ ratio is sensitive to the relative rate of exchange versus lateral diffusion, an alternative explanation is that the retardation of exchange by SH3 binding is negligible, and the higher contribution of exchange is due to the slower diffusion mediated by the SH3-inactivating mutation.

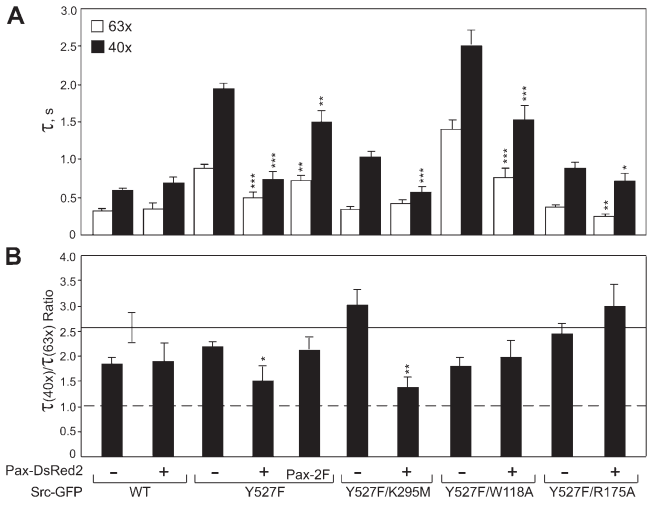

Figure 6. **FRAP studies on the effects of paxillin-DsRed2 on Src membrane interactions.** COS-7 cells were transfected with Src-GFP and paxillin-DsRed2 or paxillin-Y31F/Y118F-DsRed2 (Pax-2F; 1:10 DNA ratio) as indicated in B. Coexpressing cells were selected by their fluorescence and subjected to FRAP studies on Src-GFP as in Fig. 4. Results are mean ± SEM of 40–60 measurements. The R_f values were high in all cases (≥0.92; not depicted). (A) τ values. Asterisks indicate significant differences between the τ(63×) or τ(40×) values, comparing cells expressing Src-GFP alone versus cells coexpressing Src-GFP and paxillin-DsRed2 (*, $P < 0.05$; **, $P < 0.001$; ***, $P < 10^{-7}$). (B) τ(40×)/τ(63×) ratios. Statistical analysis comparing the effects of paxillin expression on the τ ratios of specific Src-GFP proteins (Src-GFP alone vs. Src-GFP coexpressed with paxillin-DsRed2 or Pax-2F) showed significant effects only for Src-Y527F and Src-Y527F/K295M coexpressed with paxillin-DsRed2 (*, $P < 0.05$; **, $P < 0.001$).

Src SH2 and SH3 domains bind pTyr proteins, whose formation depends on Src kinase activity and SH2 domain

To study the interactions of Src with its target proteins, we constructed GST fusion proteins with specific Src domains; the fusion proteins were coupled to glutathione–Sepharose beads and used to precipitate Src binding proteins from cells expressing different Src-GFP mutants (Fig. 5). The precipitated proteins were quantified by Western blotting using anti-pTyr antibodies. The specificity of precipitation by such fusion proteins, established in many previous studies, was confirmed by a comparison of the pTyr proteins in lysates and in precipitates, by the inability of GST alone to precipitate pTyr proteins, and by the ability of free pTyr to compete with precipitation by the GST-SH2 fusion (Fig. S1, available at http://www.jcb.org/cgi/content/full/jcb.200701133/DC1). Comparison between lysates of cells transfected by different Src-GFP mutants measures the abundance of pTyr proteins generated in vivo by each Src mutant. The precipitated pTyr proteins were generated mainly by the expressed Src-GFP proteins, as suggested by the low pTyr levels in cells transfected with GFP or with Src-WT-GFP (Fig. 5). The results demonstrate a requirement for Src kinase activity (compare cells expressing Src-Y527F with K295M mutants). The SH2-inactivating mutation (R175A) reduced the levels of precipitated pTyr proteins to about half of the level generated by Src-Y527F, consistent with previous findings on SH2-dependent multisite processive phosphorylation (Mayer et al., 1995; Pellicena and Miller, 2001), consistent with the FRAP results (Fig. 4) showing a mutual dependence on Src kinase activity and SH2 domain. On the other hand, Src-Y527F/W118A (inactive SH3) generated amounts of pTyr proteins similar to those of Src-Y527F (Fig. 5), in line with the reports that SH3 inactivation increases Src kinase activity (Seidel-Dugan et al., 1992; Erpel et al., 1995; Chong et al., 2005) and thus can compensate for loss of SH3 binding to substrates. The high pTyr levels generated by this mutant provide multiple pTyr sites that it can bind via its SH2 domain, providing increased interactions that can further retard the recovery (Fig. 4).

In the affinity precipitation studies, the lysate from cells transfected by a given Src-GFP mutant was divided into aliquots, each precipitated by beads coupled to a specific GST-Src domain. The highest pTyr level was in cells transfected by Src-Y527F; GST-SH2 and GST-SH3 precipitated similar amounts of pTyr proteins (Fig. 5 C, third histogram). GST-SH3/SH2 was twice as effective, whereas inactivating SH3 or SH2 compromised the pull-down capacity. This distribution was retained in cells transfected by all the Src mutants, except Src-Y527F/W118A. The pTyr proteins generated by the latter mutant are precipitated more effectively by GST-SH2 (Fig. 5 C, compare the blue bars). This may reflect preferential phosphorylation of target proteins to which the SH3-inactive Src mutant binds via its SH2 domain.

Overexpression of paxillin-DsRed2 interferes with the mobility-restricting interactions of Src-Y527F-GFP

We next examined the ability of paxillin, a peripheral membrane-associated Src substrate, to compete for binding to activated Src. We chose to overexpress paxillin, because although it is found in focal adhesions, it has a large cytoplasmic pool (see Fig. 7 B) and exhibits fast turnover between the pools (Webb et al., 2004; Digman et al., 2005). Cells were cotransfected with Src-GFP and an excess of paxillin-DsRed2 and subjected to FRAP beam-size analysis (Fig. 6). None of the FRAP parameters of Src-WT were significantly altered, in line with the low level of pTyr proteins in cells expressing Src-WT-GFP. On the other hand, τ(63×), τ(40×), and the τ ratio of Src-Y527F were strongly reduced to values resembling those of Src-WT (Fig. 6). Thus, excess paxillin appears to compete with the mobility-restricting binding of Src-Y527F to membrane protein targets, leaving Src-Y527F anchored in the membrane mainly by lipid-like interactions. This interpretation is supported by the finding that overexpression of paxillin-DsRed2 reduces the coimmunoprecipitation of Src-Y527F with FAK, a known Src substrate (Fig. S2, available at http://www.jcb.org/cgi/content/full/jcb.200701133/DC1). Moreover, mutation of the tyrosine phosphorylation sites on paxillin (paxillin-Y31F/W118F; Zaidel-Bar et al., 2007) significantly compromised the ability of the mutated paxillin-Y31F/Y118F-DsRed2 to affect the FRAP of Src-Y527F (Fig. 6). The incomplete loss of the effect is most likely due to the fact that paxillin contains not only SH2 but also SH3 binding sites (Schaller, 2001; Cary et al., 2002), which can contribute to Src binding via its SH3 domain. This notion is supported by the demonstration (Fig. 6) that inactivation of the SH3 domain in Src-Y527F/W118A, which retains an active SH2

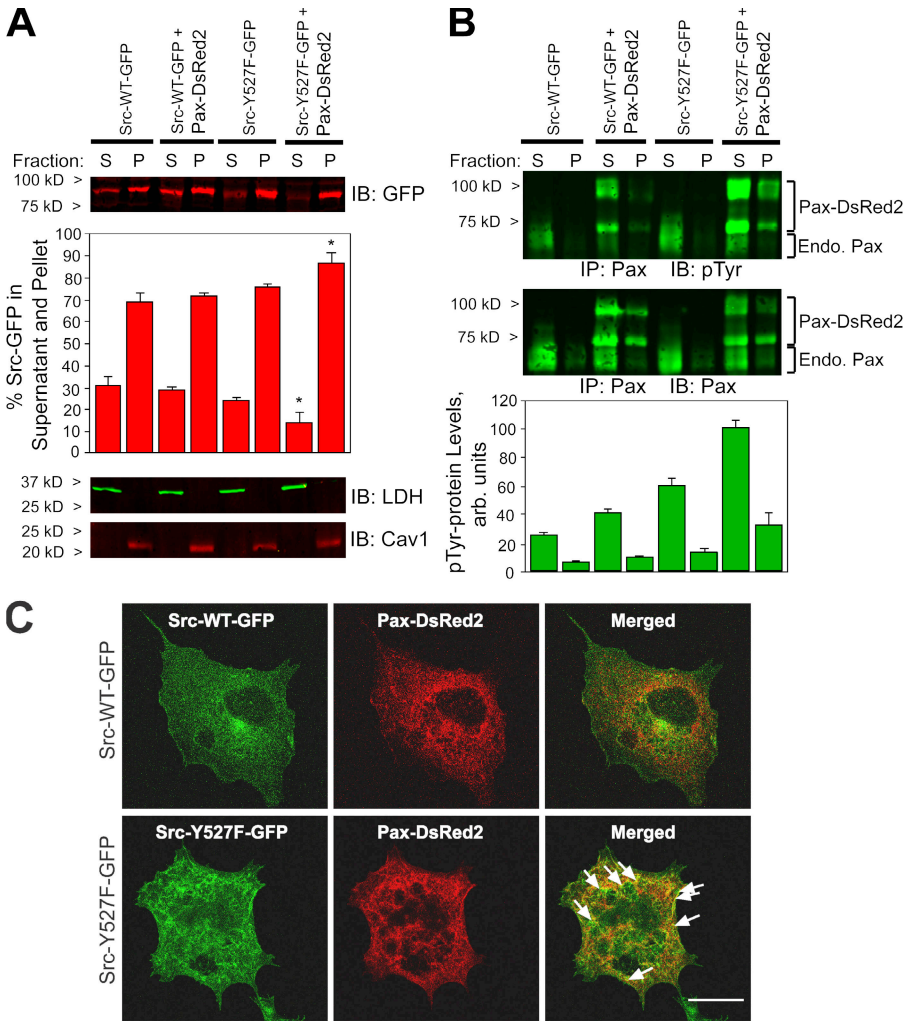

Figure 7. **Paxillin and paxillin-DsRed2 display high cytoplasmic fractions and are tyrosine phosphorylated by coexpressed Src-Y527F-GFP.** COS-7 cells were cotransfected with vectors encoding Src-WT-GFP or Src-Y527F-GFP and paxillin-DsRed2 (Pax-DsRed2) or empty vector (1:10 DNA ratio). (A) Distribution of Src-GFP between cytosolic (S) and pellet (P) fractions. Subcellular fractionation, immunoblotting, and quantification were conducted as in Fig. 1 A. The blots depict representative experiments; bars are mean ± SEM ($n = 3$) of multiple experiments. Overexpression of paxillin-DsRed2 slightly increased the percentage in pellet of Src-Y527F (*, $P < 0.05$). (B) Distribution and tyrosine phosphorylation of endogenous paxillin (Endo. Pax) and paxillin-DsRed2. Equal percentages (vol/vol) of each fraction were immunoprecipitated (IP) by anti-paxillin, followed by SDS-PAGE and immunoblotting (IB) with anti-pTyr (top) or anti-paxillin (middle; representative experiments). Bars depict means ± SEM ($n = 3$) of multiple experiments. To quantify pTyr in the paxillin and paxillin-DsRed2 bands, the sum of their intensities in each lane of the pTyr blots was calibrated according to the total paxillin level (paxillin-DsRed2 plus endogenous paxillin in both the cytosolic and pellet fractions) in the same transfection. The results are presented relative to the calibrated pTyr level precipitated from the cytosolic fraction of cells cotransfected with Src-Y527F and paxillin-DsRed2, taking this value as 100. Src-Y527F increased the levels of pTyr-paxillin and pTyr-paxillin-DsRed2 in both cytosolic and pellet to a significantly higher level than Src-WT ($P < 0.001$). (C) Cellular distribution of paxillin-DsRed2 coexpressed with Src-WT-GFP or Src-Y527F-GFP. Confocal images were obtained as in Fig. 1 B. Arrows indicate Src-GFP and paxillin-DsRed2 colocalized spots (observed for Src-Y527F-GFP but not for Src-WT-GFP). Bar, 20 μm.

domain, results in a small but distinct reduction in the ability of paxillin to affect the FRAP parameters of this Src mutant; this is shown by the lesser effect of overexpressed paxillin-DsRed2 on the τ values of Src-Y527F/W118A as compared with Src-Y527F (Fig. 6 A) and the insignificant effect on its τ(40×)/τ(63×) ratio (Fig. 6 B). The τ values of all the other Src-Y527F double mutants, which contain either kinase-dead or SH2-inactivating mutations, were only weakly affected by paxillin overexpression (Fig. 6), in line with their mainly lipid-like interactions with the membrane even in the absence of paxillin overexpression. The high sensitivity of Src-Y527F and Src-Y527F/W118A, which are the most effective in generating pTyr proteins and possess SH2 binding, to competition by paxillin is consistent with the major role of Src kinase activity and SH2 binding in the mobility-restricting interactions with membrane-associated proteins.

In accord with the requirement for Src kinase activity, kinase-dead Src-Y527F/K295M, which exhibited lipid-like membrane interactions to begin with, did not show a significant modulation in τ(63×), suggesting that D is not altered, upon expression of paxillin-DsRed2 (Fig. 6 A). However, its τ(40×) and τ(40×)/τ(63×) ratio were significantly reduced (Fig. 6), suggesting a higher contribution of exchange. This may reflect an ability of this mutant to bind paxillin via its SH3 domain, with a potential contribution of SH2 binding to pTyr-paxillin-DsRed2 generated to some degree by endogenous SFKs. The FRAP rates of Src-Y527F/R175A (inactivated SH2 domain) were only weakly affected (Fig. 6 A), consistent with SH3 binding to target proteins being much less effective than SH2 binding both in mediating mobility-restricting interactions and in competing for them.

We next examined the effects of paxillin-DsRed2 on the membrane-cytosol distribution of Src-WT and Src-Y527F (Fig. 7 A). Overexpression of paxillin-DsRed2 had no significant effects on the percentage of Src-WT-GFP in either fraction and induced a modest increase in the pellet fraction of Src-Y527F-GFP. This indicates that paxillin competition shifts Src-Y527F to membrane interactions that are mainly lipid-like, resembling Src-WT (Fig. 6). Yet, these interactions are sufficient to retain a high percentage in the particulate fraction (as observed also for Src-WT). At the same time, the ability of overexpressed paxillin to reverse the retarding interactions of activated Src with membrane proteins suggests that paxillin itself does not associate tightly with the membrane and is mainly cytoplasmic in these cells. We therefore combined subcellular fractionation with paxillin immunoprecipitation to investigate the distribution of

paxillin-DsRed2, endogenous paxillin, and their pTyr levels in cells transfected with Src-WT-GFP or Src-Y527F-GFP alone or together with paxillin-DsRed2 (Fig. 7 B). A higher percentage of paxillin and paxillin-DsRed2 was in the cytosolic fraction in cells expressing Src-WT (84% of the total paxillin and paxillin-DsRed2) and Src-Y527F (82%; Fig. 7 B, middle). pTyr-paxillin and pTyr-paxillin-DsRed2 had a similar distribution (76–81% cytosolic) in these cells. Importantly, expression of Src-Y527F-GFP as compared with Src-WT-GFP significantly increased the levels of all pTyr-paxillin proteins ($P < 0.001$; Fig. 7 B). Thus, although a fraction of paxillin is membrane associated, a major fraction is cytoplasmic, and both are subject to tyrosine phosphorylation by the coexpressed Src-Y527F-GFP. This is in accord with the ability of paxillin-DsRed2 to compete with membrane-associated Src substrates for binding Src-Y527F, and with the partial colocalization observed by confocal microscopy between the subpopulation of paxillin-DsRed2 found in clusters and Src-Y527F-GFP but not Src-WT-GFP (Fig. 7 C).

Discussion

The studies reported here indicate that Src association with the plasma membrane is dynamic and that there are major differences between the membrane interactions of Src-WT (closed conformation) and Src-Y527F (activated open conformation). We demonstrate that these differences are mediated by transient binding of Src-Y527F to target proteins in the membrane, which depend on Src kinase activity and its SH2 domain, and propose a mechanism for the regulation of Src membrane association by its specific domains.

A major fraction of Src-WT-GFP and Src-Y527F-GFP is membrane associated, but they both display significant cytosolic fractions (Fig. 1 A). This is in accord with a recent study on the SFK Lyn-GFP, which detected a fast-diffusing cytoplasmic population both before and after stimulation (Larson et al., 2005). Although the membrane fraction of Src-Y527F is only slightly higher then that of Src-WT (Fig. 1 A), their association with the membrane is very different, as indicated by the FRAP studies (Figs. 2 and 3). The lateral diffusion of Src-WT in the plasma membrane ($D \sim 0.6\ \mu m^2/s$) is close to the values measured for a lipid probe (see Results) and for the membrane-associated population of Lyn-GFP (Larson et al., 2005), suggesting that, at steady state, the large majority of Src-WT has no considerable interactions with slower-diffusing TM proteins. The Src N-terminal domain contains an *N*-myristoyl anchor and a polybasic cluster (Resh, 1999), resembling the C-terminal farnesylated lipid anchor domain of K-Ras (Hancock and Parton, 2005). In contrast, the lateral diffusion of Src-Y527F is threefold slower, implying that it is retarded by interactions with TM and/or membrane-associated proteins (Figs. 2 and 3). The biological relevance of this difference is supported by the observation that PDGF, an established activator of Src (Broome and Hunter, 1996; Abram and Courtneidge, 2000), induces a significant retardation in the FRAP kinetics of Src-WT-GFP (Fig. 3 C). This effect is smaller than the mobility retardation of the constitutively active Src-Y527F-GFP, presumably because only a fraction of the Src-WT-GFP molecules are activated by PDGF. This is in line with the modest activation of Src-WT after PDGF stimulation (Abram and Courtneidge, 2000; Sandilands et al., 2004).

The threefold slower FRAP kinetics of Src-Y527F indicate that its mobility-retarding interactions are transient (dynamic), as stable binding to target membrane proteins, which typically diffuse 10–100-fold slower than lipids (Edidin, 1992; Jacobson et al., 1995), would inhibit *D* to a much higher degree. In line with these findings, only a mild retardation of *D* was observed also for Lyn after antigen stimulation of IgE receptors (Larson et al., 2005) and for Lck after cross-linking of T cell receptors (Kusumi et al., 2005). Moreover, because the mobility-restricting interactions of Src are largely mediated by its SH2 domain (Figs. 4 and 5; discussed in the following paragraph), their dynamic nature is in accord with the report that high-affinity binding of SH2 domains to pTyr peptides is accompanied by rapid dissociation and exchange kinetics (Felder et al., 1993; Ladbury et al., 1995). The interactions of Src-Y527F with membrane proteins retard its exchange rate to an even higher degree than its lateral diffusion, as suggested by the mild increase (from 1.8 to 2.2) in the $\tau(40\times)/\tau(63\times)$ ratio (Henis et al., 2006; see Results). This correlates with the minor increase in Src-Y527F membrane association relative to Src-WT (Fig. 1 A).

To identify the Src domains responsible for the mobility-retarding interactions of constitutively active Src, we determined the effects of second mutations in Src-Y527F on the FRAP parameters (Fig. 4). The mobility retardation required both an intact SH2 domain and Src kinase activity, as shown by the shift to lipid-like diffusion (resembling Src-WT) after functional inactivation of the SH2 domain, Src kinase inactivation, or deletion of the entire catalytic segment. The SH3 domain has only a minor contribution to the mobility-restricting interactions, as its inactivation (Src-Y527F/W118A) did not eliminate the mobility retardation, which was even modestly enhanced (Fig. 4). These observations suggest that the mobility-restricting interactions of activated Src are mediated mainly by the binding of SH2 domain to pTyr residues in membrane-associated proteins. Formally, we cannot exclude the possibility that some of these pTyr residues are phosphorylated by Src-activated tyrosine kinases rather then directly by Src. However, studies with modified forms of Src that accept chemically modified nucleotides indicated that many pTyr proteins in Src-transfected cells are indeed the result of direct phosphorylation by Src (Shah et al., 1997). Thus, it appears that the modulation in Src-Y527F FRAP kinetics is mediated largely by its binding to membrane-associated protein substrates that it has itself directly phosphorylated (Fig. 8 A).

The effects of the aforementioned mutations on Src-Y527F FRAP parameters were paralleled by their effects on the abundance of pTyr proteins that can be recognized in vitro by the Src noncatalytic domains (Fig. 5). In particular, inactivation of the catalytic domain reduced the abundance of these proteins below the level observed in cells overexpressing Src-WT, and inactivation of the SH2 domain strongly reduced their level. In vitro the Src SH3 domain can bind to Src substrates (Fig. 5). However, in agreement with the dispensability of the SH3 domain for the mobility retardation of Src-Y527F, its inactivation in vivo hardly affected the abundance of the pTyr proteins (Fig. 5). The failure of the SH3 mutation to reverse the mobility

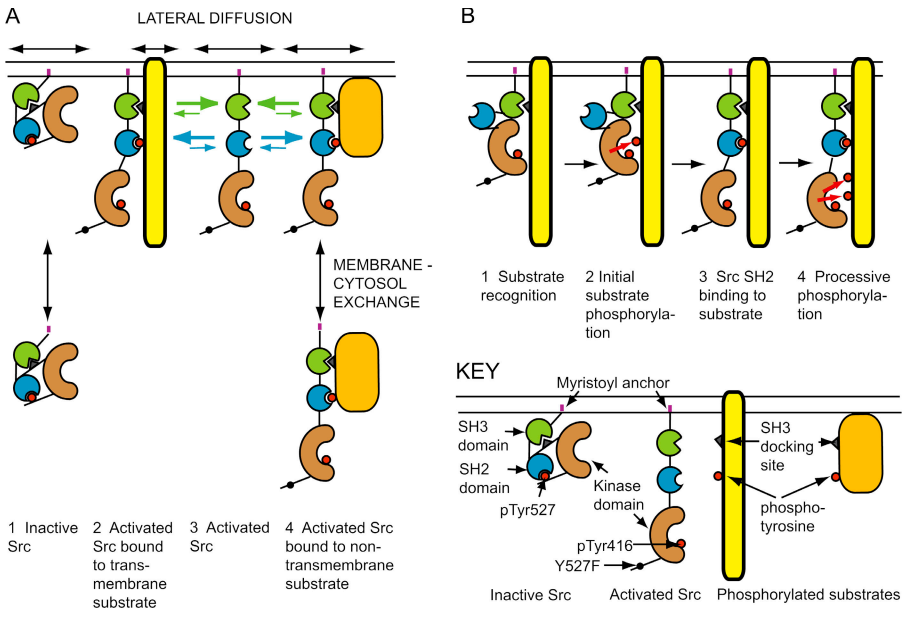

Figure 8. **Interaction of Src with its substrates.** (A) Lateral diffusion and membrane-cytosol exchange of free or substrate-bound Src. Inactive Src (1) interacts with the membrane primarily through its myristoyl anchor (purple) and the adjacent polybasic sequence and exhibits both lipid-like lateral diffusion and exchange with the cytosol. Upon activation, the open-conformation, active Src binds transiently to TM substrates, retarding its lateral diffusion and exchange (2). The mobility-retarding interactions depend mainly on SH2 domain interactions with pTyr sites (high affinity; blue arrows), with only a minor contribution of SH3 domain binding (low affinity; green arrows). Activated Src binds also to peripheral protein substrates, which compete for Src binding with the TM proteins (3 and 4). Upon binding to a peripheral protein that undergoes exchange between membrane and cytosolic pools, Src retains the N-terminal lipid-like membrane interactions; the rates of exchange and lateral diffusion of Src in complex with the peripheral protein would be affected by the membrane interactions of the latter. (B) Dependence of Src substrate phosphorylation on the Src SH2 domain: the processive multisite model. In this model, Src binds initially to the substrate (1) and phosphorylates it (red arrow; 2). This enhances the binding of Src to the substrate via its SH2 domain (3) and promotes further phosphorylation of the substrate at additional sites (processive phosphorylation; red arrows; 4). Other models that account for the SH2 dependence of Src substrate phosphorylation include protection of the pTyr residues (red circles) from pTyr protein phosphatases and targeting of Src to substrates by binding to other pTyr proteins.

inhibition indicates that in vivo the interactions of SH3 with target proteins, which are weaker than those of SH2 domains (Li, 2005; Liu et al., 2006), are too weak and labile to strongly retard the dynamic parameters. In fact, the SH3 mutation (Src-Y527F/W118A) was not simply ineffective but induced a further modest retardation in Src mobility. This can be explained by two opposing effects of SH3 inactivation. First, it can increase Src kinase activity by decreasing the inhibitory intramolecular interactions of the SH3 domain with SH2 kinase linker (Courtneidge, 2002; Frame, 2004; Chong et al., 2005). On the other hand, it decreases intermolecular interactions with SH3 binding domains in target proteins. These effects largely cancel out, but the modest additional mobility retardation after SH3 inactivation suggests that the increase in the activation of Src kinase has a higher contribution to the mobility-restricting interactions. This is in line with our conclusion that these interactions depend primarily on SH2-pTyr binding. These findings reflect what is known about the affinities of SH2 and SH3 domains. The affinity of SH2 domains to pTyr peptides is between 100 nM and 1 μM, whereas SH3 domains have weaker (micromolar) affinities for their target sites (Felder et al., 1993; Ladbury et al., 1995; Mayer, 2001).

A model for processive phosphorylation by Src was proposed based on studies with defined Src target proteins (Mayer et al., 1995; Pellicena and Miller, 2001). In this model, the relatively weak binding via the Src SH3 domain promotes initial phosphorylation of the substrate protein, leading to binding of SH2 to the resulting pTyr residue, stabilization of Src substrate interaction, and further substrate phosphorylation (Fig. 8 B). Here, we expand this model to explain the roles of Src domains in the dynamic regulation of its association with membrane sites (Fig. 8 A). We propose that Src-WT is dynamically associated with the inner membrane leaflet through lipid-like interactions (Fig. 8 A). Activated Src retains the lipid anchor interactions, but in addition, binds transiently to TM and peripheral membrane protein substrates, inhibiting its lateral diffusion and exchange. The Src SH2 domain promotes multisite processive phosphorylation (Fig. 8 B); this generates a positive feedback loop, with the SH2 domain successively promoting Src substrate binding and further phosphorylation. Although weak SH3 domain interactions may promote initial binding to substrates (Mayer et al., 1995; Pellicena and Miller, 2001), it is apparent that in cells expressing Src-Y527F, both the FRAP kinetics of active Src and the overall abundance of pTyr proteins are primarily determined by the Src SH2 domain and its interactions with pTyr sites.

Activated Src binds not only to TM proteins but also to peripheral protein substrates, which may possess a considerable cytoplasmic population. According to the model (Fig. 8 A), overexpression of such a protein should compete with the binding of activated Src to target membrane proteins. Indeed, overexpression of paxillin-DsRed2, which has a high cytosolic fraction similar to that of endogenous paxillin (Fig. 7 B), selectively interfered with the mobility retardation of Src-GFP mutants. Only Src mutants with both active kinase and intact SH2 domain were highly affected by paxillin (Fig. 6), in line with the major role of Src kinase and SH2 domain in the interactions with membrane proteins. However, although Src-Y527F reverted to lipid-like membrane association, Src-Y527F/W118A (inactivated SH3 domain) retained some mobility-retarding interactions in the presence of overexpressed paxillin, suggesting less effective competition. Because paxillin contains both SH2 and SH3 binding sites (Schaller, 2001; Cary et al., 2002), this suggests that, at least under overexpression conditions, SH3 binding partially contributes to the competition by paxillin. It should be noted that competition by paxillin did not increase the

cytoplasmic fraction of Src-Y527F, in line with the retained lipid interactions of the Src lipid anchor, which effectively targets Src-WT to the membrane (Fig. 7 A). The membrane interactions of Src–paxillin complexes may be somewhat enhanced, as indicated by the small increase in the membrane fraction of Src-Y527F after paxillin overexpression. This may reflect a contribution by the complexed paxillin to the targeting of Src to specific structures/clusters, as shown by their partial colocalization in the cells (Fig. 7 C).

The behavior of activated Src may have general implications for signaling by SFKs activated by physiological signals. Thus, the SFK Lyn was found both in the plasma membrane and the cytoplasm, and its lateral diffusion rate in the membrane was retarded after IgE receptor stimulation (Larson et al., 2005). The lateral diffusion of Lck, another SFK, was also retarded in response to cross-linking of T cell receptors (Kusumi et al., 2005). In addition, recent findings support the idea that enhanced formation of Src complexes with targets such as integrins and receptor tyrosine kinases is important for tumorigenesis (Guo et al., 2006). Thus, modulation of Src membrane interactions by binding to membrane-associated target proteins is relevant to its biological functions, including cell migration and tumorigenesis. Further characterization of these complexes by both biophysical and biochemical approaches will therefore be of considerable interest.

Materials and methods

Reagents

Murine anti-vinculin (clone hVin-1) and anti-lactate dehydrogenase (clone HH-17) ascites were obtained from Sigma-Aldrich. Murine anti-paxillin and anti-FAK were obtained from BD Biosciences. Rabbit anti-GFP and anti-caveolin1 were obtained from Santa Cruz Biotechnology, Inc. Murine anti-pTyr mAb (clone 4G10) was obtained from Upstate Biotechnology. Cy3 goat anti–mouse IgG and rabbit anti–mouse IgG were obtained from Jackson ImmunoResearch Laboratories. Goat anti–mouse IgG conjugated to IRDye 800 was obtained from Rockland Immunochemicals, and Alexa 680 goat anti–rabbit IgG was obtained from Invitrogen. *O*-phospho-L-tyrosine was obtained from Sigma-Aldrich.

Plasmids

Expression vectors for Src-WT-GFP, Src-Y527F-GFP (both in pEGFP-N1), and Src-251-GFP (in pBabePuro) (Timpson et al., 2001; Sandilands et al., 2004) were donated by M. Frame (The Beatson Institute for Cancer Research, Glasgow, Scotland). Additional Src-GFP mutants (Table I) were generated by site-directed mutagenesis using QuikChange (Stratagene). The mutagenic primers used are given in Table S1 (available at http://www.jcb.org/cgi/content/full/jcb.200701133/DC1). Constitutively active human c-Src-Y530F (prepared from molecularly cloned human c-Src; Bjorge et al., 1995) in pCI vector was a gift from D.J. Fujita (University of Calgary, Alberta, Canada). Chicken paxillin-DsRed2 in pDsRed2 (Webb et al., 2004) was donated by A.F. Horwitz (University of Virginia, Charlottesville, VA). This vector was used as a template to generate the paxillin-Y31F/Y118F-DsRed2 double mutant by site-directed mutagenesis (QuikChange), using primers 5′-GAGGAAACGCCTTTCTCCTACCCAACTGG-3′ (forward) and 5′-CCAGTTGGGTAGGAGAAAGGCGTTTCCTC-3′ (reverse) for the Y31F mutation (underlined); the Y118F mutation was added to this mutant using primers 5′-GTGAGGAGGAACACGTGTTCAGCTTCCC-3′ (forward) and 5′-GGGAAGCTGAACACGTGTTCCTCCTCAC-3′ (reverse).

Cell culture and transfections

COS-7 cells (American Type Culture Collection) were grown in DME containing 10% FCS as described previously (Shvartsman et al., 2003). For FRAP and confocal microscopy, COS-7 cells grown on glass coverslips were transfected using DEAE-dextran (Seed and Aruffo, 1987) with plasmid DNA encoding one of the Src-GFP derivatives alone or together with a 10-fold excess of paxillin-DsRed2 or empty pDsRed2. For biochemical studies, the procedure was similar, except that cells were grown in 10-cm dishes and transfected using Lipofectamine 2000 (Invitrogen).

FRAP

COS-7 cells expressing Src-GFP proteins were taken for FRAP studies 24–48 h after transfection. Measurements were in HBSS supplemented with 20 mM Hepes, pH 7.2. In some experiments, cells were first subjected to starvation in serum-free DME (16–20 h), followed by a 10-min incubation at 37°C with or without 50 ng/ml PDGF (rhPDGF-BB; R & D Systems). To minimize internalization, FRAP measurements were at 22°C, replacing samples within 15 min. An argon ion laser beam (Innova 70C; Coherent) was focused through a fluorescence microscope (Universal; Carl Zeiss MicroImaging, Inc.) to a Gaussian spot of 0.85 ± 0.02 μm (63× oil-immersion objective) or 1.36 ± 0.04 μm (40× objective), and experiments were conducted with each beam size (beam-size analysis; Illenberger et al., 2003; Henis et al., 2006). The ratio between the illuminated areas was 2.56 ± 0.30 (n = 39). After a brief measurement at monitoring intensity (488 nm, 1 μW), a 5-mW pulse (5–10 ms) bleached 60–75% of the fluorescence in the spot, and recovery was followed by the monitoring beam. The apparent characteristic fluorescence recovery time τ and the mobile fraction (R_f) were extracted from the FRAP curves by nonlinear regression analysis, fitting to a lateral diffusion process (Petersen et al., 1986).

Fluorescence confocal microscopy

Transfected cells were fixed with 4% PFA in PBS. For antibody labeling, they were permeabilized with 0.2% Triton X-100 and immunostained as detailed in the specific figure legend. The cells were mounted with Prolong Antifade (Invitrogen). Fluorescence images were collected on a confocal microscope (LSM 510; Carl Zeiss MicroImaging, Inc.) with plan-apochromat 100×/1.4 objective using LSM 510 (version 3.2 sp2) software and exported to Photoshop (Adobe).

Cell fractionation

COS-7 cells were grown and transfected with Src-GFP vectors (alone or together with paxillin-DsRed2) as described. After 24 h, the cells were suspended in hypotonic buffer (10 mM Hepes, pH 7.4, 10 mM KCl, 3 mM $MgCl_2$, 1 mM EDTA, 20 mM NaF, and 10 mM β-glycerophosphate) containing protease inhibitors (174 μg/ml PMSF, 1.5 μg/ml benzamidine, 1 μg/ml phenanthroline, 0.5 μg/ml antipain, 0.5 μg/ml leupeptin, 0.5 μg/ml pepstatin, 0.5 μg/ml aprotinin, and 0.5 μg/ml chymostatin) and subjected to Dounce homogenization. After removal of nuclei and cell debris by low-speed centrifugation, particulate and soluble fractions were separated by centrifugation (106,000 *g*, 1 h, 4°C). Particulate fractions were solubilized in a high-salt buffer (50 mM Hepes, pH 7.4, 250 mM KCl, 1.0% NP-40, 1 mM EDTA, 20 mM NaF, 10 mM β-glycerophosphate, and 5% glycerol) containing the protease inhibitors; 4× concentrated high-salt buffer was added to the soluble fractions (3:1, vol/vol). Equal proportions of the particulate and soluble fractions (5%, vol/vol) were analyzed by SDS-PAGE and immunoblotting. Blots were quantified using an imaging system (Odyssey IR; LI-COR) as detailed in the Immunoblotting section.

Construction and expression of GST fusion proteins with Src domains

To generate GST-Src domain DNA constructs, the DNA sequences encoding each domain were amplified by PCR and cloned into the pGEX-KG vector (Guan and Dixon, 1991). For plasmids encoding GST-SH3 (amino acids 79–147 of chicken c-Src), GST-SH2 (amino acids 148–251), and GST-SH3/SH2 (amino acids 79–251), Src-Y527F-GFP in pEGFP served as template. Plasmids encoding GST-SH3*/SH2 (containing a W118A SH3-inactivating mutation) and GST-SH3/SH2* (containing an R175A SH2-inactivating mutation) were generated similarly, except that Src double mutants in pEGFP (Src-Y527F/W118A-GFP and Src-Y527F/R175A-GFP, respectively) served as template. The primers used are detailed in Table S2 (available at http://www.jcb.org/cgi/content/full/jcb.200701133/DC1). Forward and reverse primers contained a BamHI site and a HindIII site, respectively (Table S2). After digestion of the PCR product and the pGEX-KG vector with these enzymes, they were ligated to generate the pGEX-Src domain vectors. All constructs were confirmed by sequencing. Bacteria transformed by the above plasmids were grown, sonicated, and lysed as described previously (Tian and Martin, 1997). The lysate from 8 ml bacteria was rocked (1 h; 4°C) with 120 μl (packed volume) of glutathione–Sepharose 4B beads (GE Healthcare). The beads were pelleted, washed five times, and stored for short periods on ice in PBS containing 0.25% Tween 20 and the protease inhibitor cocktail described in the Cell fractionation section.

GST fusion protein binding to pTyr-bearing proteins

At 48–72 h after transfection, COS-7 cells expressing specific Src-GFP proteins were lysed in NP-40 lysis buffer (50 mM Tris, pH 7.4, 150 mM NaCl, 5 mM EDTA, 1% NP-40, 50 mM NaF, and 200 μM Na_3VO_4) containing the protease inhibitors. Lysates were clarified by centrifugation, and aliquots (0.5 mg protein) were incubated for 1.5 h at 4°C with glutathione–Sepharose beads bearing ~30 μg of GST fusion protein (GST, GST-SH3, GST-SH2, GST-SH3/SH2, GST-SH3*/SH2, or GST-SH3/SH2*; described in Table S2). After four washes in lysis buffer, proteins bound to the beads were solubilized by boiling in SDS sample buffer, resolved by 8.5% SDS-PAGE, and analyzed by immunoblotting using anti-pTyr antibodies.

Immunoprecipitation

COS-7 cells cotransfected by Src-WT-GFP or Src-Y527F-GFP and paxillin-DsRed2 (or empty vector) were fractionated as described. 5% (vol/vol) of each fraction (soluble and particulate) in the high-salt buffer was taken to determine Src-GFP levels. The remaining 95% was immunoprecipitated by 1.8 μg mouse anti-paxillin essentially as described previously (Donaldson et al., 2000). Immunoprecipitation of endogenous FAK was performed similarly on whole cell lysates using 2 μg mouse anti-FAK mAb. The beads were washed three times with the high-salt buffer. Bound material was solubilized in SDS sample buffer, resolved by SDS-PAGE, and immunoblotted with anti-pTyr or anti-paxillin antibodies.

Immunoblotting

Blots were blocked in Odyssey blocking buffer (OBB; LI-COR) diluted 1:1 with PBS and incubated (12 h; 4°C) with primary antibodies (1 μg/ml anti-pTyr, 0.4 μg/ml anti-GFP, 0.25 μg/ml anti-paxillin, 0.25 μg/ml anti-FAK, and 1:500 dilution of anti-lactate dehydrogenase ascites or 0.2 μg/ml anti-caveolin1) in OBB containing 0.2% Tween 20. They were then incubated (1 h, 22°C) with secondary antibodies (0.1 μg/ml goat anti–mouse or 0.2 μg/ml goat anti–rabbit IgG coupled to IR dyes) in OBB containing 0.2% Tween 20 and 0.01% SDS. The blots were quantified using the Odyssey IR imaging system (LI-COR).

Online supplemental material

Table S1 lists the primers used to generate double and triple chicken c-Src mutants. Table S2 depicts the pGEX-KG plasmids encoding GST-Src domain fusion proteins and the primers used to generate them. Fig. S1 shows that GST-Src domain fusion proteins specifically precipitate pTyr proteins from lysates of cells expressing Src-GFP mutants. Fig. S2 shows that overexpression of paxillin-DsRed2 reduces the coimmunoprecipitation of Src-Y527F with FAK. Online supplemental material is available at http://www.jcb.org/cgi/content/full/jcb.200701133/DC1.

This work was supported by an award from the Jacqueline Seroussi Memorial Foundation for Cancer Research (to Y.I. Henis) and by National Institutes of Health grant CA17542 and a Laboratory Directed Research and Development (LDRD) Award from the Lawrence Berkeley National Laboratory (to G.S. Martin). J.C. Donaldson was supported by a National Research Service Award, and D.E. Shvartsman acknowledges support by the Joan and Jaime Constantiner Institute for Molecular Genetics. Support by the facilities of the University of California, Berkeley, Cancer Research Laboratory is acknowledged. Y.I. Henis is an incumbent of the Zalman Weinberg Chair in Cell Biology, and G.S. Martin is an incumbent of the Richard and Rhoda Goldman Chair in Cell and Developmental Biology.

We thank M. Frame, A.F. Horwitz, and D.J. Fujita for plasmid constructs and M.J. Bissell for her role as a matchmaker.

Submitted: 25 January 2007
Accepted: 12 July 2007

References

Abram, C.L., and S.A. Courtneidge. 2000. Src family tyrosine kinases and growth factor signaling. *Exp. Cell Res.* 254:1–13.

Bjorge, J.D., C. Bellagamba, H.C. Cheng, A. Tanaka, J.H. Wang, and D.J. Fujita. 1995. Characterization of two activated mutants of human pp60c-src that escape c-Src kinase regulation by distinct mechanisms. *J. Biol. Chem.* 270:24222–24228.

Bjorge, J.D., A. Jakymiw, and D.J. Fujita. 2000. Selected glimpses into the activation and function of Src kinase. *Oncogene.* 19:5620–5635.

Broome, M.A., and T. Hunter. 1996. Requirement for c-Src catalytic activity and the SH3 domain in platelet-derived growth factor BB and epidermal growth factor mitogenic signaling. *J. Biol. Chem.* 271:16798–16806.

Buss, J.E., M.P. Kamps, K. Gould, and B.M. Sefton. 1986. The absence of myristic acid decreases membrane binding of p60src but does not affect tyrosine protein kinase activity. *J. Virol.* 58:468–474.

Cary, L.A., R.A. Klinghoffer, C. Sachsenmaier, and J.A. Cooper. 2002. Src catalytic but not scaffolding function is needed for integrin-regulated tyrosine phosphorylation, cell migration, and cell spreading. *Mol. Cell. Biol.* 22:2427–2440.

Chen, Y., Y.R. Thelin, B. Yang, S.L. Milgram, and K. Jacobson. 2006. Transient anchorage of cross-linked glycosyl-phosphatidylinositol–anchored proteins depends on cholesterol, Src family kinases, caveolin, and phosphoinositides. *J. Cell Biol.* 175:169–178.

Chong, Y.P., K.K. Ia, T.D. Mulhern, and H.C. Cheng. 2005. Endogenous and synthetic inhibitors of the Src-family protein tyrosine kinases. *Biochim. Biophys. Acta.* 1754:210–220.

Courtneidge, S.A. 2002. Role of Src in signal transduction pathways. *Biochem. Soc. Trans.* 30:11–17.

Digman, M.A., C.M. Brown, P. Sengupta, P.W. Wiseman, A.R. Horwitz, and E. Gratton. 2005. Measuring fast dynamics in solutions and cells with a laser scanning microscope. *Biophys. J.* 89:1317–1327.

Donaldson, J.C., P.J. Dempsey, S. Reddy, A.H. Bouton, R.J. Coffey, and S.K. Hanks. 2000. Crk-associated substrate p130(Cas) interacts with nephrocystin and both proteins localize to cell-cell contacts of polarized epithelial cells. *Exp. Cell Res.* 256:168–178.

Edidin, M. 1992. Translational diffusion of membrane proteins. *In* The structure of biological membranes. P. Yeagle, editor. CRC Press, Boca Raton, FL. 539–572.

Erpel, T., G. Superti-Furga, and S.A. Courtneidge. 1995. Mutational analysis of the Src SH3 domain: the same residues of the ligand binding surface are important for intra- and intermolecular interactions. *EMBO J.* 14:963–975.

Felder, S., M. Zhou, P. Hu, J. Urena, A. Ullrich, M. Chaudhuri, M. White, S.E. Shoelson, and J. Schlessinger. 1993. SH2 domains exhibit high-affinity binding to tyrosine-phosphorylated peptides yet also exhibit rapid dissociation and exchange. *Mol. Cell. Biol.* 13:1449–1455.

Frame, M.C. 2004. Newest findings on the oldest oncogene; how activated src does it. *J. Cell Sci.* 117:989–998.

Guan, K.L., and J.E. Dixon. 1991. Eukaryotic proteins expressed in *Escherichia coli*: an improved thrombin cleavage and purification procedure of fusion proteins with glutathione S-transferase. *Anal. Biochem.* 192:262–267.

Guo, W., Y. Pylayeva, A. Pepe, T. Yoshioka, W.J. Muller, G. Inghirami, and F.G. Giancotti. 2006. Beta 4 integrin amplifies ErbB2 signaling to promote mammary tumorigenesis. *Cell.* 126:489–502.

Hancock, J.F., and R.G. Parton. 2005. Ras plasma membrane signalling platforms. *Biochem. J.* 389:1–11.

Henis, Y.I., B. Rotblat, and Y. Kloog. 2006. FRAP beam-size analysis to measure palmitoylation-dependent membrane association dynamics and microdomain partitioning of Ras proteins. *Methods.* 40:183–190.

Illenberger, D., C. Walliser, J. Strobel, O. Gutman, H. Niv, V. Gaidzik, Y. Kloog, P. Gierschik, and Y.I. Henis. 2003. Rac2 regulation of phospholipase C-β_2 activity and mode of membrane interactions in intact cells. *J. Biol. Chem.* 278:8645–8652.

Jacobson, K., E.D. Sheets, and R. Simson. 1995. Revisiting the fluid mosaic model of membranes. *Science.* 268:1441–1442.

Janes, P.W., S.C. Ley, A.I. Magee, and P.S. Kabouridis. 2000. The role of lipid rafts in T cell antigen receptor (TCR) signalling. *Semin. Immunol.* 12:23–34.

Kamps, M.P., and B.M. Sefton. 1986. Neither arginine nor histidine can carry out the function of lysine-295 in the ATP-binding site of p60src. *Mol. Cell. Biol.* 6:751–757.

Kamps, M.P., S.S. Taylor, and B.M. Sefton. 1984. Direct evidence that oncogenic tyrosine kinases and cyclic AMP-dependent protein kinase have homologous ATP-binding sites. *Nature.* 310:589–592.

Kamps, M.P., J.E. Buss, and B.M. Sefton. 1985. Mutation of NH2-terminal glycine of p60src prevents both myristoylation and morphological transformation. *Proc. Natl. Acad. Sci. USA.* 82:4625–4628.

Kanner, S.B., A.B. Reynolds, H.C. Wang, R.R. Vines, and J.T. Parsons. 1991. The SH2 and SH3 domains of pp60src direct stable association with tyrosine phosphorylated proteins p130 and p110. *EMBO J.* 10:1689–1698.

Kaplan, K.B., K.B. Bibbins, J.R. Swedlow, M. Arnaud, D.O. Morgan, and H.E. Varmus. 1994. Association of the amino-terminal half of c-Src with focal adhesions alters their properties and is regulated by phosphorylation of tyrosine 527. *EMBO J.* 13:4745–4756.

Kusumi, A., H. Ike, C. Nakada, K. Murase, and T. Fujiwara. 2005. Single-molecule tracking of membrane molecules: plasma membrane compartmentalization and dynamic assembly of raft-philic signaling molecules. *Semin. Immunol.* 17:3–21.

Ladbury, J.E., M.A. Lemmon, M. Zhou, J. Green, M.C. Botfield, and J. Schlessinger. 1995. Measurement of the binding of tyrosyl phosphopeptides to SH2 domains: a reappraisal. *Proc. Natl. Acad. Sci. USA.* 92:3199–3203.

Larson, D.R., J.A. Gosse, D.A. Holowka, B.A. Baird, and W.W. Webb. 2005. Temporally resolved interactions between antigen-stimulated IgE receptors and Lyn kinase on living cells. *J. Cell Biol.* 171:527–536.

Lee, H., D.S. Park, X.B. Wang, P.E. Scherer, P.E. Schwartz, and M.P. Lisanti. 2002. Src-induced phosphorylation of caveolin-2 on tyrosine 19. Phosphocaveolin-2 ($Tyr(P)^{19}$) is localized near focal adhesions, remains associated with lipid rafts/caveolae, but no longer forms a high molecular mass hetero-oligomer with caveolin-1. *J. Biol. Chem.* 277:34556–34567.

Li, S.S. 2005. Specificity and versatility of SH3 and other proline-recognition domains: structural basis and implications for cellular signal transduction. *Biochem. J.* 390:641–653.

Liu, B.A., K. Jablonowski, M. Raina, M. Arce, T. Pawson, and P.D. Nash. 2006. The human and mouse complement of SH2 domain proteins—establishing the boundaries of phosphotyrosine signaling. *Mol. Cell.* 22:851–868.

Martin, G.S. 2001. The hunting of the Src. *Nat. Rev. Mol. Cell Biol.* 2:467–475.

Mayer, B.J. 2001. SH3 domains: complexity in moderation. *J. Cell Sci.* 114:1253–1263.

Mayer, B.J., H. Hirai, and R. Sakai. 1995. Evidence that SH2 domains promote processive phosphorylation by protein-tyrosine kinases. *Curr. Biol.* 5:296–305.

Melkonian, K.A., A.G. Ostermeyer, J.Z. Chen, M.G. Roth, and D.A. Brown. 1999. Role of lipid modifications in targeting proteins to detergent-resistant membrane rafts. Many raft proteins are acylated, while few are prenylated. *J. Biol. Chem.* 274:3910–3917.

Mukherjee, A., L. Arnaud, and J.A. Cooper. 2003. Lipid-dependent recruitment of neuronal Src to lipid rafts in the brain. *J. Biol. Chem.* 278:40806–40814.

Musacchio, A., M. Saraste, and M. Wilmanns. 1994. High-resolution crystal structures of tyrosine kinase SH3 domains complexed with proline-rich peptides. *Nat. Struct. Biol.* 1:546–551.

Pellicena, P., and W.T. Miller. 2001. Processive phosphorylation of p130Cas by Src depends on SH3-polyproline interactions. *J. Biol. Chem.* 276:28190–28196.

Petersen, N.O., S. Felder, and E.L. Elson. 1986. Measurement of lateral diffusion by fluorescence photobleaching recovery. *In* Handbook of Experimental Immunology. D.M. Weir, L.A. Herzenberg, C.C. Blackwell, and L.A. Herzenberg, editors. Blackwell Scientific Publications, Edinburgh. 24.21–24.23.

Resh, M.D. 1999. Fatty acylation of proteins: new insights into membrane targeting of myristoylated and palmitoylated proteins. *Biochim. Biophys. Acta.* 1451:1–16.

Robbins, S.M., N.A. Quintrell, and J.M. Bishop. 1995. Myristoylation and differential palmitoylation of the HCK protein-tyrosine kinases govern their attachment to membranes and association with caveolae. *Mol. Cell. Biol.* 15:3507–3515.

Rotblat, B., I.A. Prior, C. Muncke, R.G. Parton, Y. Kloog, Y.I. Henis, and J.F. Hancock. 2004. Three separable domains regulate GTP-dependent association of H-ras with the plasma membrane. *Mol. Cell. Biol.* 24:6799–6810.

Sandilands, E., C. Cans, V.J. Fincham, V.G. Brunton, H. Mellor, G.C. Prendergast, J.C. Norman, G. Superti-Furga, and M.C. Frame. 2004. RhoB and actin polymerization coordinate Src activation with endosome-mediated delivery to the membrane. *Dev. Cell.* 7:855–869.

Schaller, M.D. 2001. Paxillin: a focal adhesion-associated adaptor protein. *Oncogene.* 20:6459–6472.

Schlaepfer, D.D., C.R. Hauck, and D.J. Sieg. 1999. Signaling through focal adhesion kinase. *Prog. Biophys. Mol. Biol.* 71:435–478.

Seed, B., and A. Aruffo. 1987. Molecular cloning of the CD2 antigen, the T-cell erythrocyte receptor, by a rapid immunoselection procedure. *Proc. Natl. Acad. Sci. USA.* 84:3365–3369.

Seidel-Dugan, C., B.E. Meyer, S.M. Thomas, and J.S. Brugge. 1992. Effects of SH2 and SH3 deletions on the functional activities of wild-type and transforming variants of c-Src. *Mol. Cell. Biol.* 12:1835–1845.

Shah, K., Y. Liu, C. Deirmengian, and K.M. Shokat. 1997. Engineering unnatural nucleotide specificity for Rous sarcoma virus tyrosine kinase to uniquely label its direct substrates. *Proc. Natl. Acad. Sci. USA.* 94:3565–3570.

Shenoy-Scaria, A.M., D.J. Dietzen, J. Kwong, D.C. Link, and D.M. Lublin. 1994. Cysteine3 of Src family protein tyrosine kinase determines palmitoylation and localization in caveolae. *J. Cell Biol.* 126:353–363.

Shvartsman, D.E., M. Kotler, R.D. Tall, M.G. Roth, and Y.I. Henis. 2003. Differently-anchored influenza hemagglutinin mutants display distinct interaction dynamics with mutual rafts. *J. Cell Biol.* 163:879–888.

Superti-Furga, G., and S. Gonfloni. 1997. A crystal milestone: the structure of regulated Src. *Bioessays.* 19:447–450.

Tansey, M.G., R.H. Baloh, J. Milbrandt, and E.M. Johnson Jr. 2000. GFRα-mediated localization of RET to lipid rafts is required for effective downstream signaling, differentiation, and neuronal survival. *Neuron.* 25:611–623.

Tian, M., and G.S. Martin. 1997. The role of the Src homology domains in morphological transformation by v-src. *Mol. Biol. Cell.* 8:1183–1193.

Timpson, P., G.E. Jones, M.C. Frame, and V.G. Brunton. 2001. Coordination of cell polarization and migration by the Rho family GTPases requires Src tyrosine kinase activity. *Curr. Biol.* 11:1836–1846.

Veracini, L., M. Franco, A. Boureux, V. Simon, S. Roche, and C. Benistant. 2006. Two distinct pools of Src family tyrosine kinases regulate PDGF-induced DNA synthesis and actin dorsal ruffles. *J. Cell Sci.* 119:2921–2934.

Waksman, G., S.E. Shoelson, N. Pant, D. Cowburn, and J. Kuriyan. 1993. Binding of a high affinity phosphotyrosyl peptide to the Src SH2 domain: crystal structures of the complexed and peptide-free forms. *Cell.* 72:779–790.

Webb, D.J., K. Donais, L.A. Whitmore, S.M. Thomas, C.E. Turner, J.T. Parsons, and A.F. Horwitz. 2004. FAK-Src signalling through paxillin, ERK and MLCK regulates adhesion disassembly. *Nat. Cell Biol.* 6:154–161.

Zaidel-Bar, R., R. Milo, Z. Kam, and B. Geiger. 2007. A paxillin tyrosine phosphorylation switch regulates the assembly and form of cell-matrix adhesions. *J. Cell Sci.* 120:137–148.